



## Performance analysis of two industrial dryers (cross flow and rotary) for ligno-cellulosic biomass desiccation

Nadia Cairo<sup>1</sup>, Gianpiero Colangelo<sup>1</sup>, Giuseppe Starace<sup>1</sup>

<sup>1</sup>Università del Salento

Dipartimento di Ingegneria dell'Innovazione

Via per Monteroni, Lecce

Phone number: +390832297752, e-mail: nadiacairo@libero.it, gianpiero.colangelo@unisalento.it,  
giuseppe.starace@unisalento.it

### Abstract.

Artificial drying, using industrial devices (*dryers*), helps to reduce the residual humidity content in biomass in a relatively short time. Convection is one of the most common mode of drying (referred to as *direct drying*). Heat is supplied by hot air/gas flowing over the surface of the solid. The heat for evaporation is supplied by convection to the exposed surface of the material; the evaporated humidity is carried away by the drying fluid. *Indirect dryers* (working by conduction) are more appropriate for particulate and granular materials or for very wet solids; while *radiative dryers* use various sources of electromagnetic radiation with wavelengths ranging from the infrared to microwaves.

In this work, two mathematical models of cross flow and rotary dryers (both *convective dryers*) have been proposed. Both dryers treat wood chips. The two models allow to calculate the thermal efficiency and residence time of wet solid wood chips, as a function of the residual moisture content, as well as the analysis of the behaviour of the outlet wet solid and drying gas, in consideration of the dryer length and of the feeding material conditions in the dryer. The models have been developed in the Mathcad software environment.

### Key words

Biomass, cross flow dryer, rotary dryer, wood chips, drying rate.

## 1. Introduction

### A. General considerations and state of the art

Ligno-cellulosic biomass such as wood, waste and residues of vegetal origin are the most common among those used for energy purposes. The increase in energy demand and the need to reduce greenhouse gases in the atmosphere drive to exploit this resource that could cover 14% of the Italian energy demand [1].

If the biomass is wet, the evaporation of the water absorbs part of the available energy, reducing the efficiency of the system. The wet biomass is subjected to a rapid fungi and bacteria corruption and its combustion produces volatile hydrocarbons. For this reasons, it is important to provide a curing time of the biomass to reduce its humidity content.

This work examines the drying methods involving the use of devices that can control temperature, humidity, pressure and ventilation during the entire process. Compared to the natural desiccation, consisting in leaving for a long time the biomass at open air, a lot of economic, environmental and operational advantages suggest to use these devices [2].

Industrial dryers can be classified [3] depending either on the heat transfer, or on the mode of handling the material to be dried, or on the continuity of the process. The choice of a particular configuration is determined by the size, moisture content and type of treated biomass.

In literature, several models have been developed to analyze the behaviour of a dryer in steady state conditions [3].

### B. Input-output models.

The model [3] consists basically of balancing all inputs and outputs of a dryer and it is performed to identify heat losses, calculate performance and all the most important energy parameters of a dryer. Input-output model is suitable when both the phases are perfectly mixed.

### C. Distributed parameters models.

1. **Co-current or counter-current flow.** The equations governing the mass and energy balances, both in the solid and in the gas phases, together with a suitable drying rate and heat flux equations, are solved, where all the boundary conditions (i.e., all the parameters of incoming streams) are defined [3].
2. **Cross flow.** The model [3] is based on the assumption that the solid phase has one-dimensional motion and that the drying gas and the wet biomass flows are perpendicular. Schematic of an element of the dryer length with finite thickness  $\Delta l$  is shown in Figure 3.

Based on the previous assumptions, the governing equations of mass and energy balances can be written.

Mass balance for the solid phase:

$$W_S \frac{dx}{dt} = -w_D a_V S \quad (1)$$

Energy balance for the solid phase:

$$W_S \frac{di_m}{dl} = (q - w_D h_{Av}) a_V S \quad (2)$$

Mass balance for the gas phase:

$$\frac{1}{S} \frac{dW_B(Y_2 - Y_1)}{dl} = w_D a_V \quad (3)$$

Energy balance for the gas phase:

$$\frac{1}{S} \frac{dW_B(i_{g2} - i_{g1})}{dl} = -(q - w_D h_{Av}) a_V \quad (4)$$

The drying rate and the heat flux are governed by the equations:

$$w_D = k_Y \Delta Y_m \quad (5)$$

$$q = \alpha \Delta t_m \quad (6)$$

In order to solve Equation 3 and Equation 4, a uniform distribution of gas over the whole length of the dryer is assumed, and therefore:

$$\frac{dW_B}{dt} = \frac{W_B}{L} \quad (7)$$

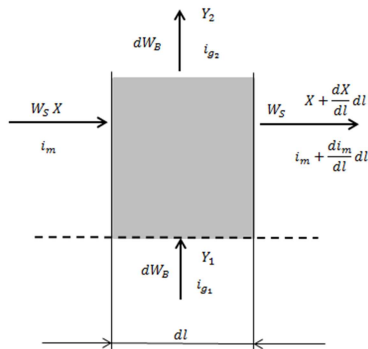


Figure 3 Element of a cross flow dryer, [3].

## 2. The new model

A new modified model, based on the cross flow distributed parameters model, assuming that the solid phase has one-dimensional motion, has been created.

The input parameters are:

- the geometric characteristics of dryer,
- the flow rate and the inlet temperature of drying gas and wet solid;
- the desired residual moisture content;
- the thermodynamic properties of the biomass (specific heat, density, porosity and critical moisture content).

The original model [4] dealt with either granular or fluid biomass. The new one simulates materials with a higher granulometric distribution, such as wood chips. These new needs lead to take into consideration other parameters. The key parameters calculated with the original model were:

- the saturation vapour pressure and the latent heat of vaporization respectively through [3], [5] the Antoine's equation:

$$\ln p_S = A - \frac{B}{c+t} \Rightarrow p_S(t) = e^{A - \frac{B}{c+t}} \quad (8)$$

And the Watson's equation (the constants values can be found in Table 1):

$$\Delta h_v = H(t - t_{ref})^n \quad (9)$$

- the relative humidity of the gas-liquid-solid system expressed as a function of temperature and humidity of the solid through the equation:

$$\varphi(t, X) = e^{\left[ \frac{-z_0}{z_2+t+t_0} e^{-z_1 X} \right]} - e^{\frac{-z_0}{z_2+t+t_0}} \quad (10)$$

valid for  $\varphi < 1$ , where  $z_0, z_1, z_2$  are the GAB equation constants. Under saturation conditions, when the partial vapour pressure in the gas equals the vapour pressure in the liquid ( $\varphi = 1$ ), the saturated absolute humidity can be expressed with the following

$$Y_S(t) = \frac{M_A p_S(t)}{M_B P_0 - p_S(t)} \quad (11)$$

and the latent heat of vaporization under saturation conditions is function of the relative humidity at constant moisture content of the solid:

$$\Delta h_S(t, X) = -\frac{R}{M_A} \left[ \frac{d \ln \varphi}{d(1/T)} \right]_{X=const} \quad (12)$$

- the wet bulb temperature  $t_{wb}$  is determined with [2]:
- $$\frac{t_g - t_{wb}}{Y - Y_S(t_{wb})} = -\frac{\Delta h_v(t_{wb})}{c_A Y + c_B} \quad (13)$$
- the absolute humidity at equilibrium, that must be lower than the saturation one to let the gas remain in the wet condition not reaching the super-saturation, is calculated through:

$$Y_r(t, X) = \frac{M_A \varphi p_S}{M_B P_0 - \varphi p_S} \quad (14)$$

The moisture content of the solid can vary in the range between the initial moisture of the solid  $X_I$  and a minimum, called equilibrium moisture content,  $X_r$ . From  $X_I$ ,  $\varphi$  (and thus  $Y_r$ ) and the critical moisture content  $X_c$ ;  $X_r$  can be calculated as follows [6]:

$$X_r(t_g, Y) = \begin{cases} 0 & \text{if } z < 0 \end{cases} \quad (15)$$

where  $z$  comes from the calculation of the zeros of the function  $f(t, \varphi) = (Y_r(t, X) - Y)$  by varying  $X$  in a fixed interval where the function goes through the X-axis.

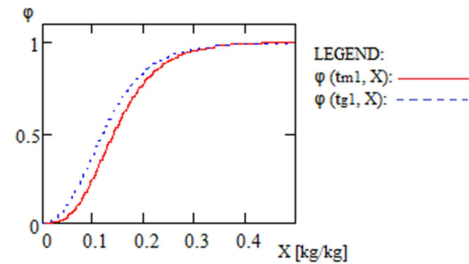


Figure 4 Trends of relative humidity for the input solid temperature ( $t_{m1}$ ) and for the inlet gas temperature ( $t_{g1}$ ) vs. moisture content ( $X$ )

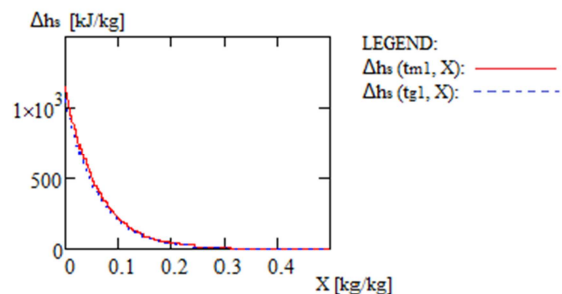


Figure 5 Trends of latent heat of vaporization for the solid temperature ( $t_{m1}$ ) and for the gas temperature ( $t_{g1}$ ) vs. moisture content ( $X$ )

The changes made to the original model introduce:

- the calculation of the porosity  $\varepsilon$  of the wood (neglecting the influence of the saturation water)[7]:
 
$$\varepsilon = 1 - \frac{\rho_p}{1530} \quad (16)$$
- the following additional assumptions (to get the mixture thermodynamic characteristics with psychrometric relations):
  - the inert gas is insoluble in the liquid phase;
  - the gas behaves as an ideal gas;
  - the liquid phase is incompressible;
  - components do not react chemically.
- determination of parameters such as [3], [5]:
  - the diffusivity of water vapour in the gas (equal to the ratio between the thermal energy transferred by conduction and the stored energy):

$$D_{AB} = D_{AB0} \left(\frac{T}{t_0}\right)^{1.75} \quad (17)$$

where:

$D_{AB0}$  is the diffusivity of water vapour in the air under conditions of total temperature and pressure ( $t_0$  and  $p_0$ )

$$T = \frac{t_{m1} + t_{g1}}{2} + t_0 \quad (18)$$

- the Reynolds ( $Re$ ) and the Schmidt ( $Sc$ ) numbers [8], through which the Sherwood number ( $Sh$ ) [6] is calculated:

$$Sh = \begin{cases} 0.91 \cdot Re^{0.49} \cdot Sc^{0.33} \cdot \psi & \text{if } Re < 50 \\ 0.61 \cdot Re^{0.59} \cdot Sc^{0.33} \cdot \psi & \text{otherwise} \end{cases} \quad (19)$$

- the drying rate:
  - in the constant-rate period ( $X_c \leq X \leq X_1$ ):

$$w_{DI} = k_Y [Y_r(t_m, X) - Y] \quad (20)$$

-in the falling-rate period ( $X_r \leq X \leq X_c$ ):

$$w_D = w_{DI} \left(\frac{X - X_r}{X_c - X_r}\right)^n \quad (21)$$

where:  $n$  is the dimensionless constant in the equation of the characteristic curve of drying;

- the energy efficiency of the dryer:

$$\eta = \frac{E_{ev}}{E_t} \quad (22)$$

where:  $E_{ev}$  is the energy used for moisture evaporation at the solids feed temperature and  $E_t$  is the total energy supplied to the dryer.

For convective drying, that occurs at a constant specific heat and low humidity and temperature values, the energy and thermal efficiency can be confused [2]:

$$\eta_T = \frac{t_{g1} - t_{g2}}{t_{g1} - t_{amb}} \quad (23)$$

$$\eta_{Tmax} = \frac{t_{g1} - t_{wb}}{t_{g1} - t_{amb}} \quad (24)$$

- for the cross-flow dryer, the equations to determine the mass and energy balance are [6], [9]:

$$\frac{dX}{dl} = -\frac{B \cdot H}{W_S} \cdot w_D \cdot a_V \quad (25)$$

$$\frac{di_m}{dl} = \frac{B \cdot H \cdot a_V}{W_S} \cdot (q - w_D h_A) \quad (26)$$

$$\frac{dY}{dl} = \frac{B \cdot H}{W_B} \cdot w_D \cdot a_V \quad (27)$$

$$\frac{di_g}{dl} = -\frac{B \cdot H \cdot a_V}{W_B} \cdot (q - w_D h_A) \quad (28)$$

where

$$h_A = c_A + t_m \Delta h_{v0} \quad (29)$$

$$a_V = \frac{B \cdot L}{B \cdot L \cdot H} \quad (30)$$

while the residence time of the wet solid inside the dryer comes from two contributions:

$$\theta_t = \theta_c + \theta_f \quad (31)$$

where

$$\theta_c = (X_1 - X_c) \cdot \frac{\rho_v \Delta h_S}{a a_V (t_g - t_m)} \quad \text{if } X_c \leq X \leq X_1 \quad (32)$$

and

$$\theta_f = \frac{-4H^2}{D_{AB}\pi^2} \cdot \ln\left(\frac{X - X_r}{X_c - X_r}\right) \quad \text{if } X_r \leq X \leq X_c \quad (33)$$

- for the co-current rotary dryer without flights, a new set of mass and energy balance that becomes [10]:

$$\frac{dX}{dl} = -\frac{(Set - At)}{W_S} \cdot w_D \cdot a_V \quad (34)$$

$$\frac{di_m}{dl} = \frac{(Set - At) \cdot a_V}{W_S} \cdot (q - w_D h_A) \quad (35)$$

$$\frac{dY}{dl} = \frac{(Set - At)}{W_B} \cdot w_D \cdot a_V \quad (36)$$

$$\frac{di_g}{dl} = -\frac{(Set - At) \cdot a_V}{W_B} \cdot (q - w_D h_A) \quad (37)$$

where

$$a_V = \frac{bL}{(Set - At)L} \quad (38)$$

The residence time of the wet solid expressed in seconds from

$$\theta = \frac{0.310 \cdot (L \cdot n_1)^{0.5}}{D \cdot N_1 \cdot \delta} \cdot 3600 \quad (39)$$

The drying rate determines the behavior of the solid during drying by measuring the loss of moisture content versus time [2]. Figure 7.a shows the data for the moisture content  $W$  (dry basis) as a function of time  $\theta$ . This curve represents the evaporation of moisture from a wet solid. Figure 6.a shows that the drying rate varies with the time or the moisture content, these changes are better illustrated in the diagrams 7.b and 7.c.

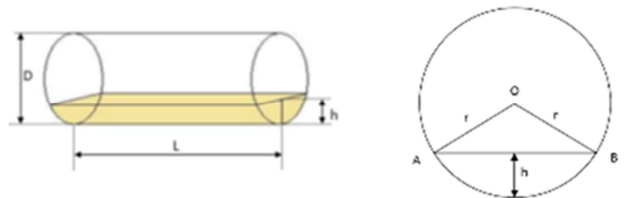


Figure 6 Schematic view of the dryer loading and front view of the rotary dryer

Table 1 Coefficients of the approximation equation for WATER

PROPERTY	SYMBOL	UNIT	VALUE
Molar mass	$M_A$	kg kmol <sup>-1</sup>	18.01
Saturated vapor pressure	$A$	kPa	16.38
Coefficient	$B$	kPaK <sup>-1</sup>	3878.82
Coefficient	$C$	K	229.86
Heat of vaporization	$H$	kJkg <sup>-1</sup>	352.58
Reference temperature	$t_{ref}$	K	374.14
Coefficient	$n$		0.33

The distance AB on each curve represents the "warm-up period" of solid, BC the "constant-rate period". The point C, where the drying rate begins to decrease, is called "critical moisture content". The part of the curve

CD is called "falling-rate period" and here a continuous speed change during the rest of the drying cycle can be observed. At the point E all the exposed surface becomes completely unsaturated and here starts the part of the drying cycle during which the internal movement of moisture controls the speed of drying. The CE portion is called the "first falling-rate period" while the portion DE is called "second falling-rate period."

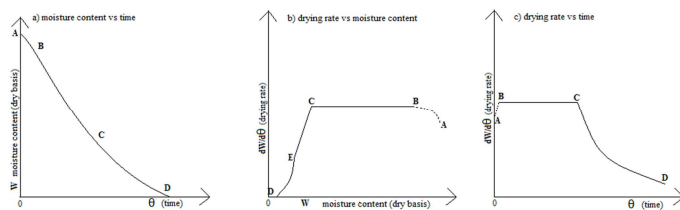


Figure 7 Periods of drying, [2].

After its revision, the model has been adapted to the actual operating conditions, selecting appropriate design parameters. A Mathcad 14 routine, was implemented to investigate the effects of operating parameters changes.

The biomass used in the calculations was oak or fir chips of size 5×5×20 cm, with an initial moisture content of 50%. Each element of wood chips was modeled as a series of spheres of diameter  $d = 5$  cm and correction factor  $\psi = 0.89$  was considered to make the assumptions consistent.

The coefficient  $\psi$  is a parameter defined by the ratio between the actual outer surface of the element of wood chips and the outer surface of the equivalent sphere (the sphere with the same volume of the wood chip). Relevant properties are reported in Table 2 [11]. The drying gas can vary the flow rate and inlet temperature, while remaining unchanged features are reported in Table 3 [2].

Table 2 Properties of WOOD BIOMASS

PROPERTY	UNIT	OAK	FIR
Specific heat $c_s$	$\text{kJ kg}^{-1}\text{K}^{-1}$	4.53	4.968
Density $\rho_s$	$\text{kg m}^{-3}$	850	450
Critical moisture content $X_C$	$\text{kg}_v \cdot \text{kg}_{\text{solid}}^{-1}$	0.4	0.31

Table 3 Thermodynamic constants and properties of WET GAS

PROPERTY	UNIT	VALUE
Specific heat of water vapour $c_A$	$\text{kJ kg}^{-1}\text{K}^{-1}$	1.8
Specific heat of dry air $c_B$	$\text{kJ kg}^{-1}\text{K}^{-1}$	1.02
Gas density $\rho_g$	$\text{kg m}^{-3}$	1.2
Initial gas moisture $Y_i$	$\text{kg}_v \cdot \text{kg}_a^{-1}$	0.002
Dynamic viscosity of gas $\mu_g$	$\text{Pa s}$	$18.6 \times 10^{-6}$
Diffusivity of water vapour $D_{ABO}$	$\text{m}^2\text{s}^{-1}$	$20 \times 10^{-6}$

With reference to the cross-flow and rotary dryers, the selected dryers have the characteristics given in Table 4 [12] and Table 5 [13] respectively.

Table 4 Dimensions of the CROSS-FLOW DRYER

CHARACTERISTIC	UNIT	VALUE
Model		VIBRO-FLUIDIZER 9
Length	$\text{m}^{-3}$	10000
Width	$\text{m}^{-3}$	900
Height of the bed*	$\text{m}^{-3}$	200

\* This value must be less than  $250 \text{ m}^{-3}$  for a uniform drying

Table 5 Dimensions of the ROTARY DRYER

CHARACTERISTIC	UNIT	VALUE
Model		ZL50-16-I
Length	$\text{m}^{-3}$	8000
Width	$\text{m}^{-3}$	100
Height of the bed	$\text{m}^{-3}$	30
Slope of the dryer	$\text{m} \cdot \text{m}^{-1}$	0.026
Dynamic angle of repose of the solids	deg	39.85
Electric power	kW	3.28
Dryer weight	kg	7490

#### 4 Results and discussion

The dryer performance is measured in terms of thermal efficiency and residence time of the wet material inside it. For both dryers (rotary and cross-flow), some influent parameters have been highlighted that modify the behaviour of the wet solid and drying gas. These parameters were:

- drying gas temperature;
- drying gas flow rate;
- drying gas velocity;
- final moisture content.

In tables 6 and 7, for both dryers, the main results of the simulations with the new model are summarized. In particular: in CASE I oak chips were used; in CASE II the dryer was fed with fir chips; in CASE III and CASE IV the drying gas inlet temperature and flow rate have been increased.

No similar simulations for wood chips were found in literature.

With regard to performance, cross-flow dryer residence times were found significantly lower than in rotary dryer. The graphs in Table 6 represent the results of the simulations of the four cases, where the trends of humidity and temperature as a function of the distance travelled by the material inside the cylinder of the dryer have been examined. The performance of the oak wood chips is quite acceptable in terms of residence time and efficiency of the dryer (Table 6). To reach the desired moisture content, about 2 minutes and 34 seconds are needed, covering about 9.52 m inside the dryer.

Comparing the first two cases, it is clear that the model is sensitive to the different chips used to feed the dryer. Fir wood chips, characterized by value of critical and equilibrium moisture contents lower than in the oak wood chips (Tables 2 and 6) achieve a higher performance..

Comparing the CASE I and CASE III for oak wood chips (see Table 6) a reduction in drying time from 154.6 s to 122.8 s is evident, as well as an increasing of the gas

temperature from 130 °C to 160 °C. This shows the influence of the drying gas temperature.

Table 6 Results of the simulation for the CROSS FLOW dryer

PROPERTY	UNIT	CASES			
		I	II	III	IV
INPUT DATA					
Wet biomass flow rate	$\text{kg s}^{-1}$	0.1	0.1	0.1	0.1
Drying gas flow rate	$\text{kg s}^{-1}$	4	4	4	7
Biomass temperature	°C	20	20	20	20
Gas temperature*	°C	130	140	160	130
Residual moisture content	$\text{kg}_v \text{kg}_{\text{solid}}^{-1}$	0.2	0.2	0.2	0.2
OUTPUT DATA					
Equilibrium moisture content	$\text{kg}_v \text{kg}_{\text{solid}}^{-1} \cdot 10^{-3}$	2.5	1.6	0.33	2.5
Mass transfer coefficient gas-solid	$\text{kg s}^{-1} \text{m}^{-2}$	0.201	0.168	0.207	0.201
Heat transfer coefficient	$\text{WK}^{-1} \text{m}^{-2} \cdot 10^3$	206	172	172	206
Wet bulb temperature	°C	37.1	38.5	41.2	37.01
Dryer length	m	9.5	9.6	6.6	7.1
Gas moisture*	$\text{kg}_v \text{kg}_{\text{d a}}^{-1}$	0.017	0.017	0.017	0.011
Gas temperature*	°C	77.7	85.2	102.4	99.6
Biomass temperature*	°C	46.6	44.0	51.4	49.1
Residence time*	s	154.6	89.5	122.8	120.0
Thermal efficiency*		0.50	0.48	0.50	0.29
Max thermal efficiency*		0.89	0.88	0.89	0.89

\* values function of the distance traveled inside the dryer

Increasing the drying gas flow rate for oak wood chips from 4 kg/s to 7 kg/s, a performance degradation on the dryer can be observed: the thermal efficiency becomes 30% (Table 6).

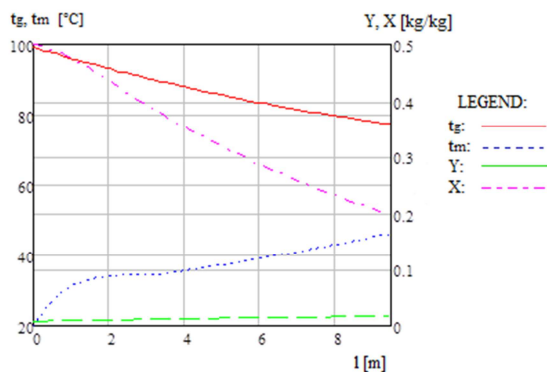


Figure 8 Trends of gas ( $t_g$ , Y) and solid ( $t_m$ , X) temperatures and moisture vs. length of the cross flow dryer. CASE I

Table 7 Results of the simulations for the ROTARY dryer

PROPERTY	UNIT	CASES			
		I	II	III	IV
INPUT DATA					
Wet biomass flow rate	$\text{kg s}^{-1}$	0.1	0.1	0.1	0.1
Drying gas flow rate	$\text{kg s}^{-1}$	3	3	3	7
Biomass temperature	°C	20	20	20	20
Gas temperature	°C	165	165	175	165
Residual moisture content	$\text{kg}_v \text{kg}_{\text{solid}}^{-1}$	0.2	0.2	0.2	0.2
OUTPUT DATA					
Equilibrium moisture content	$\text{kg}_v \text{kg}_{\text{solid}}^{-1} \cdot 10^{-4}$	2.0	6.7	0.47	2.0
Mass transfer coefficient gas-solid	$\text{kg s}^{-1} \text{m}^{-2}$	0.12	0.12	0.12	0.12
Heat transfer coefficient	$\text{kWK}^{-1} \text{m}^{-2}$	0.12	0.12	0.12	0.12
Wet bulb temperature	°C	41.8	41.8	43.0	41.8
Dryer length	m	7.9	7.7	7.1	5.2
Gas moisture*	$\text{kg}_v \text{kg}_{\text{d a}}^{-1} \cdot 10^{-3}$	22	22	22	11
Gas temperature*	°C	88.1	86.7	95.8	131.1
Biomass temperature*	°C	50.1	45.9	51.5	54.6
Residence time*	s	1541	1516	1458	1242
Thermal efficiency*		0.55	0.55	0.53	0.24
Max thermal efficiency*		0.88	0.88	0.88	0.88

\* values function of the distance traveled inside the dryer

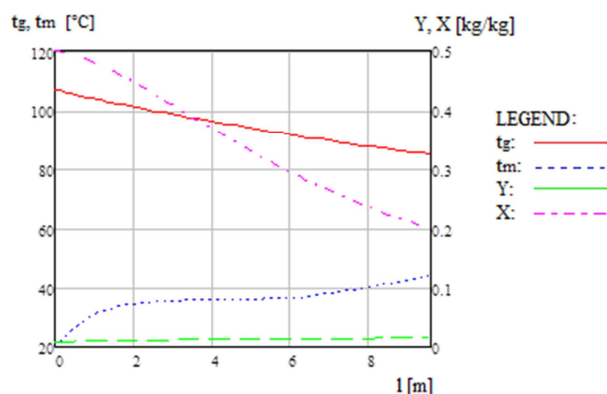


Figure 9 Trends of gas ( $t_g$ , Y) and solid ( $t_m$ , X) temperatures and moisture vs. length of the cross flow dryer. CASE II

In the rotary dryer, thermal efficiency were observed higher than those of the cross-flow one but, at the same time, an increase of the drying time. The case here

commented inform that the variation of the critical parameters affected both the dryers at the same way. Charts are built on the basis of the results of Table 7.

The fir wood chips are characterized by critical and equilibrium moisture contents lower than those of the oak chips; for this reason slightly better performance both in terms of thermal efficiency and in drying time required can be achieved.

For oak wood chips, increasing the temperature of the gas has a positive influence on drying time (CASE I vs. CASE III). The thermal efficiency shows low values, about 24%, by increasing the drying gas flow rate. This effect makes the decrease in drying time useless.

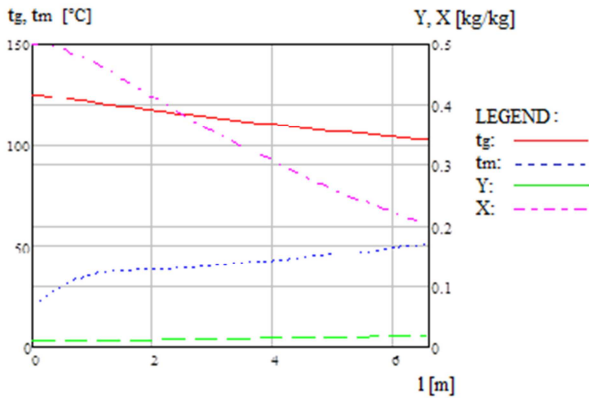


Figure 10 Trends of gas ( $t_g$ ,  $Y$ ) and solid ( $t_m$ ,  $X$ ) temperatures and moisture vs. length of the cross flow dryer. CASE III

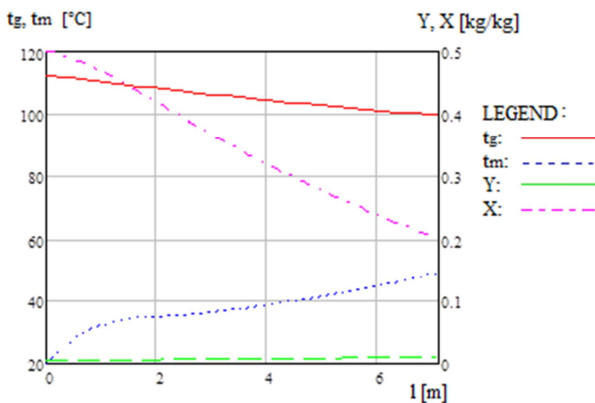


Figure 11 Trends of gas ( $t_g$ ,  $Y$ ) and solid ( $t_m$ ,  $X$ ) temperatures and moisture vs. length of the cross flow dryer. CASE IV

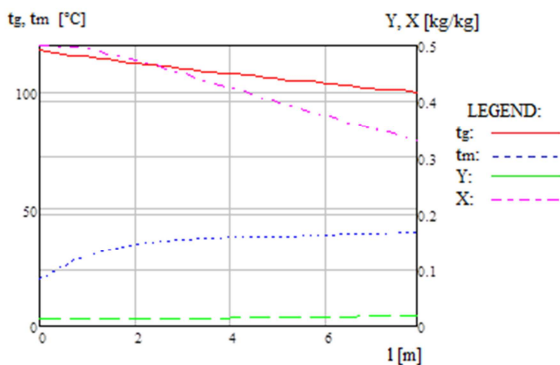


Figure Trends of gas ( $t_g$ ,  $Y$ ) and solid ( $t_m$ ,  $X$ ) temperatures and moisture vs. length of the cross rotary dryer. CASE I

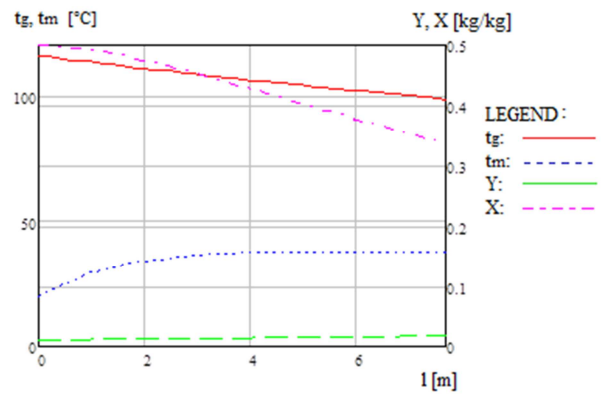


Figure 13 Trends of gas ( $t_g$ ,  $Y$ ) and solid ( $t_m$ ,  $X$ ) temperatures and moisture vs. length of the cross rotary dryer. CASE II

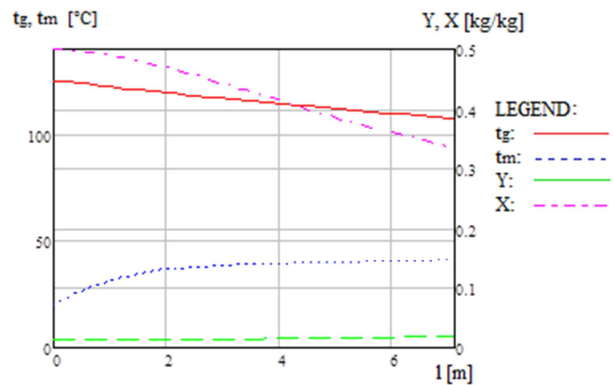


Figure 14 Trends of gas ( $t_g$ ,  $Y$ ) and solid ( $t_m$ ,  $X$ ) temperatures and moisture vs. length of the cross rotary dryer. CASE III

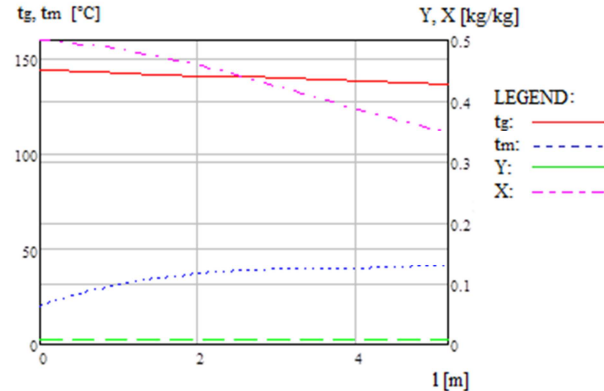


Figure 15 Trends of gas ( $t_g$ ,  $Y$ ) and solid ( $t_m$ ,  $X$ ) temperatures and moisture vs. length of the cross rotary dryer. CASE IV

## 5 Conclusions

The potential of two types of industrial dryers (rotary and cross-flow) or the drying of wood chips was analyzed. The available biomass was made of oak and fir, size:  $5 \times 5 \times 20$  cm. The desired residual moisture in both cases was 20%.

The simulations were carried out with in Mathcad 14 environment. The speed of the process of water removing from the material surface (drying rate) was modeled, starting from the actual moisture content of the solid. The performance evaluation of the dryers chosen was performed in terms of thermal efficiency and residence time of the wet material inside the dryer. The model

responds to the changes in temperature and flow rate of the drying gas, to the wood chips used and to the values of critical and equilibrium moisture content relevant to the biomass. In addition to these parameters, the amount of moisture to be removed and the geometric characteristics of the dryer, particularly the length of the device, affect the residence time of the wet material inside the dryer.

Based on the results and the type of biomass chosen, the best performance are those of the cross-flow dryer, especially with reference to time of drying.

The best thermal performance was found, instead, in the rotary dryer, with a worse drying time.

The model was developed for a dryer without flights; the choice of such a configuration was determined by the size and consistency of the biomass used. Gases are forced through the cylinder by either an exhauster or an exhauster/blower combination and the material characteristics determine the feeding method of the dryer, which can be done by a chute extending into the cylindrical shell or by a screw feeder.

### Acknowledgments

This work was done within the research and development project of SOCOGES srl (Monopoli - BA - Italy) with the financial support of the European Union and Regione Puglia (P.O. 2007-2013 Asse I – Linea 1.1 Aiuti agli investimenti in ricerca per le PMI - Azione 1.1.2)

### Nomenclature

$\alpha$ = heat transfer coefficient	$\text{kW} \cdot \text{K}^{-1} \text{m}^{-2}$
$\delta$ = slope of the dryer	
$\Delta h_s$ = latent heat of sorption	$\text{kJ} \cdot \text{kg}^{-1}$
$\Delta h_{v,0}$ = latent heat of vaporization at $t_0$	$\text{kJ} \cdot \text{kg}^{-1}$
$A_t$ = area of the triangle OAB	$\text{m}^{-2}$
$a_v$ = characteristic interfacial area per unit volume of dryer	$\text{m}^{-1}$
$B$ = width of the dryer	$\text{m}$
$b$ = base of the triangle OAB	$\text{m}$
$c_A$ = specific heat of water vapor	$\text{kJ} \cdot \text{kg}^{-1} \text{K}^{-1}$
$c_{A1}$ = specific heat of water	$\text{kJ} \cdot \text{kg}^{-1} \text{K}^{-1}$
$c_B$ = specific heat of dry air	$\text{kJ} \cdot \text{kg}^{-1} \text{K}^{-1}$
$c_S$ = specific heat of dry solid	$\text{kJ} \cdot \text{kg}^{-1} \text{K}^{-1}$
$H$ = height of the bed of the dryer	$\text{m}$
$i$ = specific enthalpy	$\text{kJ} \cdot \text{kg}^{-1}$
$k_Y$ = mass transfer coefficient	$\text{kg} \cdot \text{s}^{-1} \text{m}^{-2}$
$L$ = length of the dryer	$\text{m}$
$M_A$ = molar mass of water	$\text{kg} \cdot \text{kmol}^{-1}$
$M_B$ = molar mass of air	$\text{kg} \cdot \text{kmol}^{-1}$
$R$ = universal gas constant	$\text{kJ} \cdot \text{K}^{-1} \text{kmol}^{-1}$
$S$ = section area	$\text{m}^2$
$t_{wb}$ = wet bulb temperature	$\text{K}$
$V$ = total volume	$\text{m}^3$
$W_B$ = drying gas flow rate	$\text{kg} \cdot \text{s}^{-1}$
$W_S$ = wet solid flow rate	$\text{kg} \cdot \text{s}^{-1}$
$w_D$ = drying rate	$\text{kg} \cdot \text{s}^{-1} \text{m}^{-2}$
$X$ = solid moisture content	$\text{kg}_v \cdot \text{kg}_{\text{solid}}^{-1}$
$Y$ = gas absolute humidity	$\text{kg}_v \cdot \text{kg}_a^{-1}$
$Y_S$ = saturated absolute humidity	$\text{kg}_v \cdot \text{kg}_a^{-1}$

### Subscripts and superscripts

$c$	= input direct heat
$d a$	= dry air
$l$	= heat loss
$m$	= input mechanical energy
$t$	= net heat transported by the transport devices
$v$	= vapour
*	= in equilibrium

### References

- [1] Bonari, E., Pampana S. Biomasse agricole e lingo-cellulosiche. In: Baldini, S. *Biomasse agricole e forestali per uso energetico*, Agra, Roma, 2002 pp. 81-97.
- [2] Perry, R.H., Green, D.W., Perry's Chemical Engineers Handbook Seventh Edition. McGraw-Hill, printed in the USA 1999, pp. 1153-1243.
- [3] Mujumdar, A., Taylor; Francis, Handbook of Industrial Drying 3rd Ed., CRC Press 2007, pp. 4-199, 1075-1078.
- [4] Pakowski, Z.; Mujumdar, A.S. Basic Process Calculations and Simulations in Drying. CRC press 2006
- [5] Johansson, A.; Fyrh,C.; Rasmuson, A. High temperature convective drying of wood chips air. In International journal of Heat and Mass transfer vol. 40, No. 12. Elsevier Science; printed in Great Britain 1997, pp. 2843-2858
- [6] Loo,S. V., Koppejan, J., The handbook of Biomass Combustion & Co-firing, Sjaak, V.L.; Jaap, K.; printed in UK and USA 2008, pp. 7-50, 134-164
- [7] Data taken from: [www.ricercaforestale.it](http://www.ricercaforestale.it)
- [8] Cengel, Y.A. Termodinamica e trasmissione del calore. Mc Graw Hill.
- [9] Garnavi, L. Kasiri, N.; Hashemabadi, S.H. Mathematical modelling for a continuous fluidized-bed dryer. In International journal of Heat and Mass Transfer No. 33. Elsevier Science; printed in Iran 2006, pp. 666-675
- [10] Walas S.M., Chemical Process Equipment. Selection and Design, Butterworth-Heinemann Series in Chemical Engineering; printed in USA 1990, pp. 231-262
- [11] Data taken from ENEA data sheet
- [12] Data taken from data sheet for cross-flow dryers available on [www.niro.dk](http://www.niro.dk)
- [13] Data taken from data sheet for rotary dryers available on [www.dryerwood.it](http://www.dryerwood.it)